

UC Irvine

UC Irvine Previously Published Works

Title

C5aR1 signaling promotes region- and age-dependent synaptic pruning in models of Alzheimer's disease

Permalink

<https://escholarship.org/uc/item/68p1f01h>

Journal

Alzheimer's & Dementia, 20(3)

ISSN

1552-5260

Authors

Gomez-Arboledas, Angela

Fonseca, Maria I

Kramar, Enikő

et al.

Publication Date

2024-03-01

DOI

10.1002/alz.13682


Copyright Information

This work is made available under the terms of a Creative Commons Attribution License, available at <https://creativecommons.org/licenses/by/4.0/>

Peer reviewed

RESEARCH ARTICLE

C5aR1 signaling promotes region- and age-dependent synaptic pruning in models of Alzheimer's disease

Angela Gomez-Arboledas¹ | Maria I. Fonseca¹ | Enikő Kramar² | Shu-Hui Chu¹ |
Nicole D. Schartz¹ | Purnika Selvan¹ | Marcelo A. Wood² | Andrea J. Tenner^{1,2,3} 

¹Department of Molecular Biology and Biochemistry, University of California, Irvine, California, USA

²Department of Neurobiology and Behavior, University of California, Irvine, California, USA

³Department of Pathology and Laboratory Medicine, University of California, School of Medicine, Irvine, California, USA

Correspondence

Andrea J. Tenner, Department of Molecular Biology and Biochemistry, University of California, 3205 McGaugh Hall, Irvine, CA 92697-3900, USA.
Email: atenner@uci.edu

[Correction added on February 14, 2024, after first online publication: National Science Foundation in the funding information section has been corrected to NIH.

Funding information

Cancer Center Support, Grant/Award Number: CA-62203; Center for Complex Biological Systems Support, Grant/Award Number: GM-076516; NIH, Grant/Award Numbers: AG060148, AG061746, AG076835, AG054349; Larry L. Hillblom postdoctoral fellowship, Grant/Award Number: 2021-A-020-FEL; Alzheimer's Association Research Fellowship, Grant/Award Number: AARFD-20-677771; Edythe M. Laudati Memorial Fund

Abstract

INTRODUCTION: Synaptic loss is a hallmark of Alzheimer's disease (AD) that correlates with cognitive decline in AD patients. Complement-mediated synaptic pruning has been associated with this excessive loss of synapses in AD. Here, we investigated the effect of C5aR1 inhibition on microglial and astroglial synaptic pruning in two mouse models of AD.

METHODS: A combination of super-resolution and confocal and tridimensional image reconstruction was used to assess the effect of genetic ablation or pharmacological inhibition of C5aR1 on the Arctic48 and Tg2576 models of AD.

RESULTS: Genetic ablation or pharmacological inhibition of C5aR1 partially rescues excessive pre-synaptic pruning and synaptic loss in an age and region-dependent fashion in two mouse models of AD, which correlates with improved long-term potentiation (LTP).

DISCUSSION: Reduction of excessive synaptic pruning is an additional beneficial outcome of the suppression of C5a-C5aR1 signaling, further supporting its potential as an effective targeted therapy to treat AD.

KEYWORDS

Alzheimer's disease, C1q, C5aR1, LTP, microglia, synaptic pruning

Highlights

- C5aR1 ablation restores long-term potentiation in the Arctic model of AD.
- C5aR1 ablation rescues region specific excessive pre-synaptic loss.
- C5aR1 antagonist, PMX205, rescues VGlut1 loss in the Tg2576 model of AD.
- C1q tagging is not sufficient to induce VGlut1 microglial ingestion.
- Astrocytes contribute to excessive pre-synaptic loss at late stages of the disease.

This is an open access article under the terms of the [Creative Commons Attribution](https://creativecommons.org/licenses/by/4.0/) License, which permits use, distribution and reproduction in any medium, provided the original work is properly cited.

© 2024 The Authors. *Alzheimer's & Dementia* published by Wiley Periodicals LLC on behalf of Alzheimer's Association.

1 | BACKGROUND

Alzheimer's disease (AD) is a devastating neurodegenerative disorder that impairs memory and results in cognitive deficits, often accompanied by psychiatric disorders. Neuropathologically, AD is characterized by the extracellular accumulation of amyloid- β (A β) in senile plaques and neurofibrillary tangles and synaptic and neuronal loss.¹ It is also well established that inflammation and the complement system play key roles in disease progression, where glial cell responses to amyloid may contribute to neuronal damage and cognitive impairment.^{2,3} In fact, genome-wide association (GWAS) studies have identified at least three complement genes as being significantly associated with AD: *CLU*, *CR1*, and *C1S*.⁴ Activation of the classical and alternative complement pathways during AD occurs as a response to fibrillar β -sheet amyloid β (fA β) and hyperphosphorylated tau.⁵⁻⁷ Additionally, multiple complement mediators have been found to colocalize with A β plaques, not only in mouse models of the disease,^{8,9} but more importantly, in human post-mortem samples from AD patients,¹⁰⁻¹⁴ further supporting a critical role of the complement system in AD pathogenesis (reviewed in ref.¹⁵). Activation of the complement system by fibrillar A β could ultimately generate C5a, which can then interact with a proinflammatory C5aR1 receptor (which is upregulated by injury or infection) on microglial cells,^{16,17} triggering a potent inflammatory response.

During development, synapse elimination or refinement is a necessary process to ensure the appropriate establishment of synaptic circuits. The classical pathway of the complement system, through C1q and C3, has been directly linked to beneficial synaptic pruning that occurs in developmental stages, including adulthood.^{18,19} However, multiple studies implicate synaptic loss as a hallmark of AD that correlates best with the cognitive decline in AD patients.²⁰ Interestingly, complement-mediated synaptic pruning has been associated with the excessive synaptic loss that occurs during AD. It has been hypothesized that excessive complement activation could mediate aberrant synapse pruning by microglial engulfment in AD models, as well as in other neurodegenerative disorders,^{13,21-23} ultimately leading to cognitive decline.

It is known that C1q binds to phosphatidyl serine and other damage exposed molecules on apoptotic cells, and likely interacts with similar molecules at weak or nonactive synapses.^{24,25} Activation of complement at the synapses can lead to microglial engulfment of C1q/iC3b tagged synapses via CR3 receptor on microglial cells.²¹ In addition, deficiency or blockage of C1q, C3, C4, and CR3 has been shown to suppress synaptic pruning and prevent cognitive deficits in several mouse models of AD.^{13,23,26} Furthermore, evidence for a neuroprotective role for C1q suggests that upstream inhibition of the complement system might not be an optimal target to treat AD.^{27,28}

Previous studies in our lab, and others, have shown that the genetic or pharmacological inhibition of C5a-C5aR1 signaling reduced pathology, and rescued synaptic and cognitive loss in several mouse models of AD,²⁹⁻³³ suggesting that C5a-C5aR1 signaling might be a better therapeutic target than blocking the upstream components of the complement cascade. Moreover, two different C5aR1 antagonists have

RESEARCH IN CONTEXT

- 1. Systematic review:** The authors reviewed the literature using traditional (e.g., PubMed) sources and meeting abstracts and presentations. While the specific role of C5aR1 in synaptic pruning during Alzheimer's disease (AD) pathogenesis is still not fully understood, there have been several recent publications demonstrating key roles of the complement system in both synaptic pruning and AD. All these relevant citations are appropriately cited.
- 2. Interpretation:** Our findings show that suppression of C5aR1 (either by genetic ablation or pharmacological inhibition) improved long-term potentiation and rescues the excessive pre-synaptic loss in two mouse models of AD.
- 3. Future directions:** The manuscript highlights the beneficial effect of the suppression of C5a-C5aR1 signaling as a target therapy to treat AD. Further work is required to understand: (a) the specific molecular mechanism by which C5aR1 is exerting this beneficial effect; (b) the specific "eat-me" and "don't eat me" signals and/or complement regulatory molecules involved in the synaptic pruning process.

already been proven safe in humans in different clinical trials for autoimmune disorders, further emphasizing the potential for C5aR1 as a therapeutic target.^{34,35} In addition, it is well established that astrocytes play a key role in circuit refinement during development and adulthood³⁶; however, their putative role in the excessive synaptic loss observed in AD is still controversial. In a recent report, astrocytes were found to preferentially ingest excitatory synapses while microglia engulfed inhibitory synapses in mouse models of tauopathy and AD,³⁷ suggesting that astrocytes might also have an important role in synaptic pruning during AD.

Therefore, here we investigated the effect of genetic ablation or pharmacological inhibition of C5aR1 on microglial and astroglial synaptic pruning in two different mouse models of AD. We show that synaptic loss and excessive microglial synaptic pruning can be partially rescued by genetic deletion or pharmacological inhibition of C5aR1 in an age and region dependent manner.

2 | METHODS

2.1 | Animals

All animal experimental procedures were approved by the Institutional Animal Care and Use Committee of University of California, Irvine, and performed in accordance with the National Institutes of Health (NIH) Guide for the Care and Use of Laboratory Animals. The AD mouse

model Arctic48 (Arc), initially provided by Dr. Lennart Mucke (Gladstone Institute, San Francisco, CA), contains the human APP transgene with the Indiana (V717F), Swedish (K670N + M671L), and Arctic (E22G) mutations (under the control of the platelet derived growth factor- β promoter) and, thus, produces A β protofibrils and fibrils at 2-4 months old.³⁸ The C5aR1 knockout mice, generated by target deletion of the C5a receptor gene and initially provided by Dr. Rick Wetsel (University of Texas, Houston), were crossed with Arctic^{+/-} mice, kindly provided by Dr. Lennart Mucke (Gladstone Institute), to produce Arctic mice lacking C5aR1 (Arc-C5aR1KO) and wild-type (WT) littermate mice lacking the C5a receptor (C5aR1KO) (Supp Figure S1A). Tg2576 mice, developed by K. Hsiao³⁹ overexpressed the 695 isoform of the amyloid precursor protein (APP) with the Swedish mutation (KM670/671NL) under the control of the prion promoter on a B6/SJL genetic background. Only female hemizygous Tg2576 mice were used as they develop cortical amyloid plaques by 11-13 months of age, earlier than male Tg2576.³⁹ WT (B6/SJL) female littermates were used as control mice (Supp Figure S1B).

2.2 | C5aR1 antagonist (PMX205) treatment

C5aR1 antagonist, PMX205, was kindly provided by Dr. Ian Campbell, Teva Pharmaceuticals, West Chester, PA. Treatment with PMX205 was performed as previously described.³² Briefly, PMX205 was administered in the drinking water at 20 μ g/ml to mice at the onset of amyloid pathology at 12 months of age for the Tg2576 mice (and B6/SJL WT littermates) (Supp Figure S1B). PMX205 treatment was administered for 12 weeks and mice were singly housed and had free access to the drinking water during the whole treatment. Mice were single housed during the whole PMX205 treatment to calculate drug consumption for each individual mouse. Additionally, mice were also weighed weekly and, as we previously reported, showed no weight change due to treatment.³²

2.3 | Tissue collection and preparation

WT, C5aR1KO, Arc, and Arc-C5aR1KO mice at different ages (2.7, 5, 7, and 10 months old) were deeply anesthetized with isoflurane and transcardially perfused with 4% paraformaldehyde/phosphate buffered saline (PBS) and post fixed overnight in 4% paraformaldehyde/PBS at 4°C or perfused with PBS and fixed for 24 h with 4% paraformaldehyde/PBS at 4°C (no differences were seen in results from different perfusion methods). Brains were sectioned at 40 μ m using a vibratome (Leica VT 1000S). For the Tg2576 and WT littermates that underwent PMX205 treatment, mice were deeply anesthetized with isoflurane and transcardially perfused with HBSS modified buffer (Hank's balanced salt solution without calcium and magnesium), containing actinomycin D (5 μ g/ml) and Triptolide (10 μ M). Half brains were fixed in 4% paraformaldehyde for 24 hours and sectioned at 40 μ m thickness in the coronal plane on a vibratome (Leica VT1000S).

2.4 | Golgi staining and Sholl analysis

Mice were perfused as above, and half brains were fixed and, after sectioning (150 μ m), stained using the super-Golgi Kit (Bioenno Lifesciences, Santa Ana, CA), following the instructions of the manufacturer. All sections were coded, and the analysis was done blinded. The stained tissues were then quantified using a stereology Zeiss Axio Imager M2 with NeuroLucida software Version 11.03. The soma and apical dendrites along with its dendritic branching were traced under 100 \times magnification in the CA3 region of the hippocampus for each animal followed by Sholl analyses, which determines the average number of branchings for a given distance from the soma (μ m) of each neuron. The average number of branchings for a given distance from the soma for the neurons of each animal and genotype \pm SEM were generated using GraphPad Prism.

2.5 | Antibodies

The following primary antibodies were used for this study: mouse monoclonal anti-synaptophysin (SP) (clone SVP38, 1.4 μ g/ml, Sigma), guinea pig polyclonal anti VGlut1 (1:1000, Millipore), rabbit polyclonal anti postsynaptic density 95 (PSD95, 1 μ g/ml, Invitrogen), rat monoclonal anti CD68 (clone FA-11, 1.4 μ g/ml, Bio-Rad), rabbit polyclonal anti Iba-1 (1:1000, Wako), rat monoclonal anti C3 (clone 11H9, 0.5 μ g/ml, Abcam), and rabbit monoclonal anti C1q (clone 27.1, hybridoma supernatant previously described^{40,41}). The specificity of the anti-mouse C1q antibody was demonstrated by the lack of C1q staining detected in the hippocampal CA1-SR of an Arctic C1q conditional KO (ArcC1qa^{FL/FL}:Cx3cr1^{ERT2}) compared with the Arc C1qa^{FL/FL} at super-resolution level (Supp Figure S2) as characterized previously.⁴⁰

2.6 | Immunofluorescence

Coronal brain sections were blocked with 2% bovine serum albumin (BSA), 10% normal goat serum, 0.1% Triton, TBS (1 h, room temperature [RT]), and incubated with primary antibodies diluted in blocking solution overnight at 4°C. After washing, antigen-bound primary antibodies were detected with the corresponding labelled Alexa 488, Alexa 555, or Alexa 647 secondary antibodies (1/300 – 1/500, Invitrogen) that were incubated for 1 h at RT. Sections were then mounted either with ProLong glass antifade mounting media (Invitrogen) for super-resolution microscopy or with Vectashield Hardset (Vector) for confocal imaging.

2.7 | Image acquisition

For super-resolution imaging, hippocampal regions CA1-SR, DG-ML, and CA3-SL of WT, C5aR1KO, Arc, and Arc-C5aR1KO at different ages were acquired with a Zeiss LSM 880 Airyscan microscope and Zen

image acquisition software (Zeiss) with identical conditions. Images for each animal and within all the regions of interest were collected using a 63x oil objective. 3-4 Z stacks (187 nm step interval, within a depth of 3 μm , covering an area of 58 \times 58 μm) representative of the specific area were acquired. For super-resolution imaging of WT and Tg2576 mice treated with/without PMX205, hippocampal regions CA1-SR and CA3-SL were acquired by Super-Resolution Lattice Structured Illumination Microscopy (Lattice-SIM) using an Elyra 7 microscope system (Zeiss). Images for each animal and within all the regions of interest were collected using a 63 \times 1.4NA Plan-Apo objective lens and Immersol 518F immersion oil. 4 z-stacks (110 nm step interval, within a depth of 5-8 μm , covering an area of 64 \times 64 μm) per region/mouse/group were acquired to obtain a full representation of the CA1-SR or CA3-SL. Images were processed using ZEN SIM² on the ZEN black edition software. For confocal imaging of microglial/astroglial synaptic pruning, individual microglial/astroglial cell images were obtained with a Leica TCS SP8 microscope under a 63x objective and a 3.5 zoom factor. Z-stacks were acquired in 0.3 μm steps to image the whole microglial/astroglial cell. For each mouse the CA1-SR and CA3-SL regions of the hippocampus were imaged. A total of 15 cells per mouse, per region and age were acquired and analyzed, based on our previous work as well as protocols developed by others.^{23,32}

2.8 | Imaris quantitative analysis

Image analyses were carried out in several hippocampal regions by using Imaris 9.2 or 9.5 software (Bitplane Inc). In our study, we were interested in the three main hippocampal regions, CA1-SR, CA3-SL, and DG-ML that are involved in the trisynaptic circuit; however, since our previous results showed no differences at any age or genotype group on the DG-ML, in this manuscript, we focused only on CA1-SR and CA3-SL hippocampal areas. Colocalization of pre and post synaptic puncta (SP or VGlut1 with PSD95) and C1q or C3 associated with presynaptic puncta (SP or VGlut1) were quantified using the spots or the surfaces function on Imaris and Matlab software to determine the total number of colocalized spots (defined at ≤ 200 nm distance) or the number of spots close to surfaces (≤ 200 nm distance). Spots were normalized to the total image volume. Synaptic engulfment was defined as the co-localization (defined at ≤ 200 nm distance) of VGlut1+ synapses (detected by Imaris spots) with either CD68 (%VGlut1 engulfment in microglial/astroglial lysosomes) or Iba1/glial fibrillary acidic protein (GFAP) (%VGlut1 engulfment) surfaces and normalized to the total volume of the image.

2.9 | Hippocampal slice preparation and long-term potentiation recording

Hippocampal slices were prepared from male and female 10-month-old WT, Arctic, WT-C5aR1KO, and Arc-C5aR1KO mice ($n = 36$). Following isoflurane anesthesia, mice were decapitated, and the brain was quickly removed and submerged in ice-cold, oxygenated dissection

medium containing (in mM): 124 NaCl, 3 KCl, 1.25 KH_2PO_4 , 5 MgSO_4 , 26 NaHCO_3 , and 10 glucose. Coronal hippocampal slices (340 μm) were prepared using a vibratome (VT1000S) before being transferred to an interface recording containing preheated artificial cerebrospinal fluid (aCSF) of the following composition (in mM): 124 NaCl, 3 KCl, 1.25 KH_2PO_4 , 1.5 MgSO_4 , 2.5 CaCl_2 , 26 NaHCO_3 , and 10 glucose and maintained at $31 \pm 1^\circ\text{C}$. Slices were continuously perfused with this solution at a rate of 1.75-2 ml/min while the surface of the slices were exposed to warm, humidified 95% O_2 / 5% CO_2 . Recordings began following at least 2 hours of incubation.

Field excitatory postsynaptic potentials (fEPSPs) were recorded from CA1b stratum radiatum using a single glass pipette filled with 2 M NaCl (2-3 M Ω) in response to orthodromic stimulation (twisted nichrome wire, 65 μm diameter) of Schaffer collateral-commissural projections in CA1 stratum radiatum. Pulses were administered at 0.05 Hz using a current that elicited a 50% maximal response. Paired-pulse facilitation was measured at 40, 100, and 200 second intervals prior to setting baseline. After establishing a 20 min stable baseline, long-term potentiation (LTP) was induced by delivering 5 'theta' bursts, with each burst consisting of four pulses at 100 Hz and the bursts themselves separated by 200 msec (i.e., theta burst stimulation or TBS). The stimulation intensity was not increased during TBS. Data were collected and digitized by NAC 2.0 Neurodata Acquisition System (Theta Burst Corp., Irvine, CA) and stored on a disk.

2.10 | Statistics

All data were analyzed using either a t-test for comparison of two groups and one-way analysis of variance (ANOVA) or two-way ANOVA, followed by Tukey's post hoc test for comparison among more than two groups by using GraphPad Prism Version 9 (La Jolla, CA) and Microsoft Excel. The significance was set at 95% confidence. * $p < 0.05$, ** $p < 0.01$, *** $p < 0.001$, and **** $p < 0.0001$. Data were presented as the mean \pm SEM (standard error of the mean).

3 | RESULTS

3.1 | C5aR1 depletion on the Arctic model of AD restores short- and long-term plasticity at 10 months of age

Genetic ablation of C5aR1 in the Arctic mouse model of AD results in a protection from cognitive decline and from loss of neuronal complexity in the CA1²⁹ and CA3 region of the hippocampus (Supp Figure S3) at 10 months of age. To evaluate the potential contributions of C5aR1 in synaptic plasticity, the cellular mechanism believed by many to underlie memory processes, we examined long-term potentiation (LTP) in acute hippocampal slices from 10 months WT, C5aR1KO, Arctic and Arc-C5aR1KO mice. Evoked field excitatory post-synaptic potentials (fEPSPs) were recorded from the CA1b stratum radiatum hippocampal region. Following a train of theta burst stimulation (TBS) to a collection

of Schaffer-commissural fibers, fEPSP slope increased immediately and dramatically in WT slices that then decayed over the following 10 min to reach a stable level of potentiation at approximately 50% above baseline 60 minutes post-induction (Figure 1A-C). Interestingly, LTP in slices from C5aR1KO mice and Arctic mice were significantly reduced 50-60 minutes post-TBS compared to WT slices (Figure 1A-C). However, LTP in slices from Arc-C5aR1KO were indistinguishable from WT controls (Figure 1A-C). These results indicate that like the C5aR1KO mouse, the Arctic mouse model has a strong impairment in LTP, but more importantly, the deletion of C5aR1KO in the Arctic mouse model of AD can restore deficits in LTP to control levels.

We then investigated if the absence of C5aR1 affects any of the conventional measures of transmission related to short term plasticity (input/output curves and paired pulse facilitation). Input-output curves measuring the magnitude of the fEPSP slope (Figure 1D-G) and fiber volley (Figure 1E-G) in response to an increase in stimulus current were comparable for WT, C5aR1KO, and Arctic-C5aR1KO mice, but there was a marked depression of fEPSP slope in Arctic mice (Figure 1D). These results indicate that deletion of C5aR1 alone does not affect axon excitability. However, we did find that slices from the Arctic mice (relative to controls) showed depressed axon excitability and that deletion of C5aR1 from the Arctic mouse restores normal axonal transmission. We then tested for differences in transmitter release using paired pulse facilitation (PPF). Slices from C5aR1KO and Arc-C5aR1KO did not differ from WT controls (Figure 1H), but PPF in Arctic slices was significantly reduced at 40 msec stimulus interval suggesting that Arctic mice have a reduction in transmitter mobilization. Taken all together, our results showed that while the Arctic mice showed the greatest deficit in both synaptic transmission and LTP, the absence of C5aR1 appears to have restored both short- and long-term plasticity.

3.2 | Absence of C5aR1 rescues the excessive VGlut1 presynaptic puncta loss at 10 months of age in the Arctic mouse model of AD

Here, we assessed whether genetic ablation of C5aR1 would similarly dampen synaptic pruning by microglia at 10 months of age in the CA3-SL hippocampal region. Super-resolution microscopy (Figure 2A1) and Imaris quantification (Figure 2A2-A4) of VGlut1, PSD95, and VGlut1-PSD95 colocalized synaptic puncta showed a significant VGlut1 presynaptic loss (55% reduction) in the Arctic mouse model of AD (vs WT). Moreover, we observed an increase in VGlut1+ synaptic puncta in the Arc-C5aR1KO mice when compared to Arctic mice, indicative of a partial presynaptic puncta rescues when C5aR1 was depleted (Figure 2A2). No differences on any of the genotypes were observed on PSD95 postsynaptic density (Figure 2A3). Colocalization of VGlut1 and PSD95 synaptic puncta showed a significant synaptic loss (40% reduction) in the AD mice when compared to WT (Figure 2A4); however, no rescue of synaptic density was detectable. These results indicate a potential role of C5a-C5aR1 signaling in the excessive presynaptic loss associated with AD.⁴²

It has been widely reported that weak or less-active synapses associated with complement components C1q and cleaved C3 are actively engulfed by microglial cells through CR3, a receptor for the opsonic complement activation product iC3b.²¹ To determine if C1q tagging correlated with the changes observed in synaptic density, and if the presence of C1q could be used to predict vulnerable or reduced synaptic puncta, we analyzed VGlut1 and C1q immunostaining (Figure 2B1-4) in WT, C5aR1KO, Arc, and Arc-C5aR1KO mice at 10 months of age in the CA3-SL region. Quantitative analysis from super-resolution images showed a significant decrease in VGlut1 puncta in Arctic mice (compared to WT), that was partially rescued by the absence of C5aR1 (Arc-C5aR1KO vs. Arc mice) (Figure 2B2), as also seen in Figure 2A2. Additionally, we observed a significant increase (2.7-2.9-fold increase) in C1q in Arctic mice relative to WT (Figure 2B3). When assessing the colocalization of C1q with VGlut1, we observed a significant increase in C1q-VGlut1 colocalized puncta in the Arctic mice (vs. WT), which was even further increased in the Arc-C5aR1KO (although not statistically significant when compared to Arc mice) (Figure 2B4). Since VGlut1 puncta is increased in Arc-C5aR1KO (compared to Arctic mice) but there is no difference in % C1q puncta, our results suggest that although C1q tagging plays a role in presynaptic pruning in this AD mouse model, the presence of C1q puncta is not sufficient to lead to ingestion of synapses. Rather additional factors such as C5a-C5aR1 activated microglia or neurons that are more susceptible to injury (or both) are required.

C3 has been shown to be involved in synapse pruning.^{13,21,23,43} To investigate if C3 tagging would correlate with the VGlut1 presynaptic density changes observed at 10 months of age in the Arc and Arc-C5aR1KO (vs. WT) mice in the CA3-SL region, sections were immunostained for C3 and VGlut1, and quantification studies were carried out with Imaris software (Supp Figure S4). As seen in previous experiments (Figure 2A2 and 2B2), VGlut1 density was decreased in the Arc relative to WT and partially rescued in the Arc-C5aR1KO (Supp Figure S4A2). C3 staining, using an antibody that recognizes whole C3 as well as its cleavage products, was observed mainly on astrocytes and deposited on the neuropil. Our results showed a high amount of C3 positive astrocytes, mainly in the vicinity of amyloid plaques (data not shown), which parallels previous bulk RNAseq and IHC results from our lab showing a strong astroglial response (characterized by an increased in GFAP and C3) in the hippocampus of Arctic and Arc-C5aR1KO mice at 7 and 10 months of age.³³ Here, our results at 10 months in the CA3-SL region showed a significant increase of C3 puncta (excluding astroglia-associated C3) in the Arc mice when compared to WT littermates, which was further increased in the Arc-C5aR1KO mice (Supp Figure S4A3). However, no significant differences were found in the C3-VGlut1 colocalized puncta among any of the different genotypes (Supp Figure S4A4), suggesting that as with C1q, while C3 may play a role in synaptic pruning in the Arctic mouse model at 10 months of age, other factors must also be contributing substantially to the ingestion of presynaptic VGlut1.

Since complement activation at the synapses or activation by fibrillar amyloid plaques will generate C5a (when C5 is present) and since the expression of C5aR1 increases with age and pathology,¹⁶

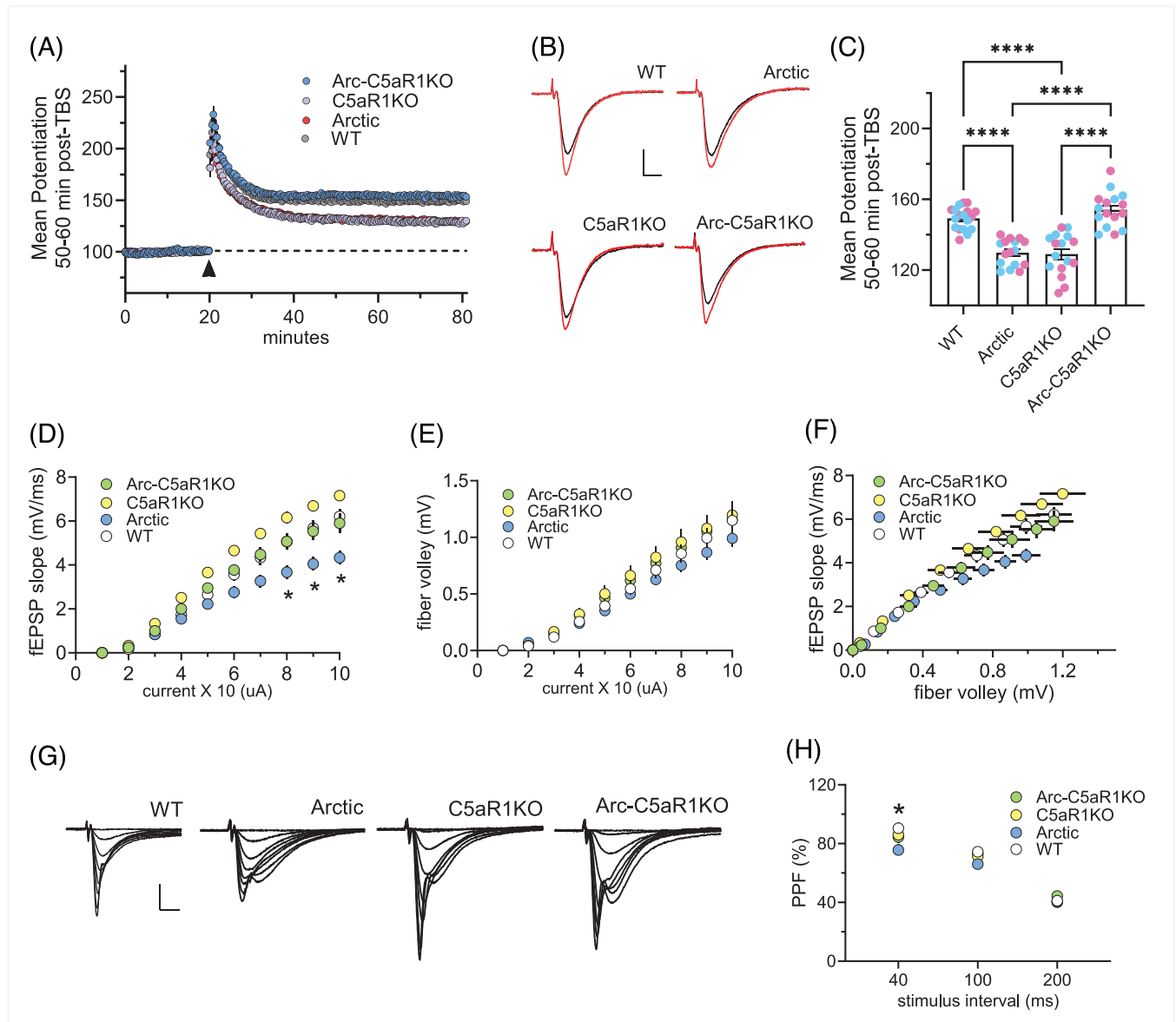


FIGURE 1 Genetic deletion of C5aR1 rescues LTP deficit in Arctic mice at 10 months of age. (A) Hippocampal slices were collected from 10-month-old (mo) male and female WT, Arctic, C5aR1KO, and Arc-C5aR1KO mice ($n = 8-9$ mice/genotype). Long-term potentiation (LTP) in the CA1-SR area was measured. Following a 20 minute stable recording, LTP was induced by applying TBS (black arrow) and recording of baseline stimulation was resumed for an additional 60 min. Immediately following TBS, fEPSP slope increased and then slowly decayed to a stable level of LTP above baseline recordings in slices from WT (grey circle), Arctic (red circle), C5aR1KO (purple circle), and Arc-C5aR1KO (blue circle) mice. (B) Representative traces collected during baseline (black line) and 60 min post-TBS (red line). Scale: 1 mV/5 ms. (C) The mean potentiation 50-60 min post-TBS was significantly impaired in Arctic and C5aR1KO mice relative to WT and Arc-C5aR1KO mice ($p < 0.0001$). Light blue and pink circles represent mean potentiation of each slice in male and female mice, respectively. (D-E) Input/output curves assessed the amplitude of the fEPSP slope (panel D) and fiber volley (panel E) across a range of stimulus currents (10-100 uA) ($*p < 0.01$). (F) Input/output curves comparing the amplitudes of the presynaptic fiber volley to the fEPSP slope across a range of stimulus currents. (G) Representative field recordings collected during the first through eight steps of the input/output curve in slices from WT, Arctic, C5aR1KO, and Arc-C5aR1KO mice. Scale: 2 mV/5 ms. (H) Paired pulse facilitation (PPF) of the initial slope of the synaptic response was compared in slices from Arc-C5aR1KO and C5aR1KO relative to WT mice, and in Arctic mice at the 40 ms stimulus interval ($p = 0.03$). $*p < 0.05$, $****p < 0.0001$ using one-way ANOVA (C) and two-way ANOVA (H) followed by Tukey's post hoc test.

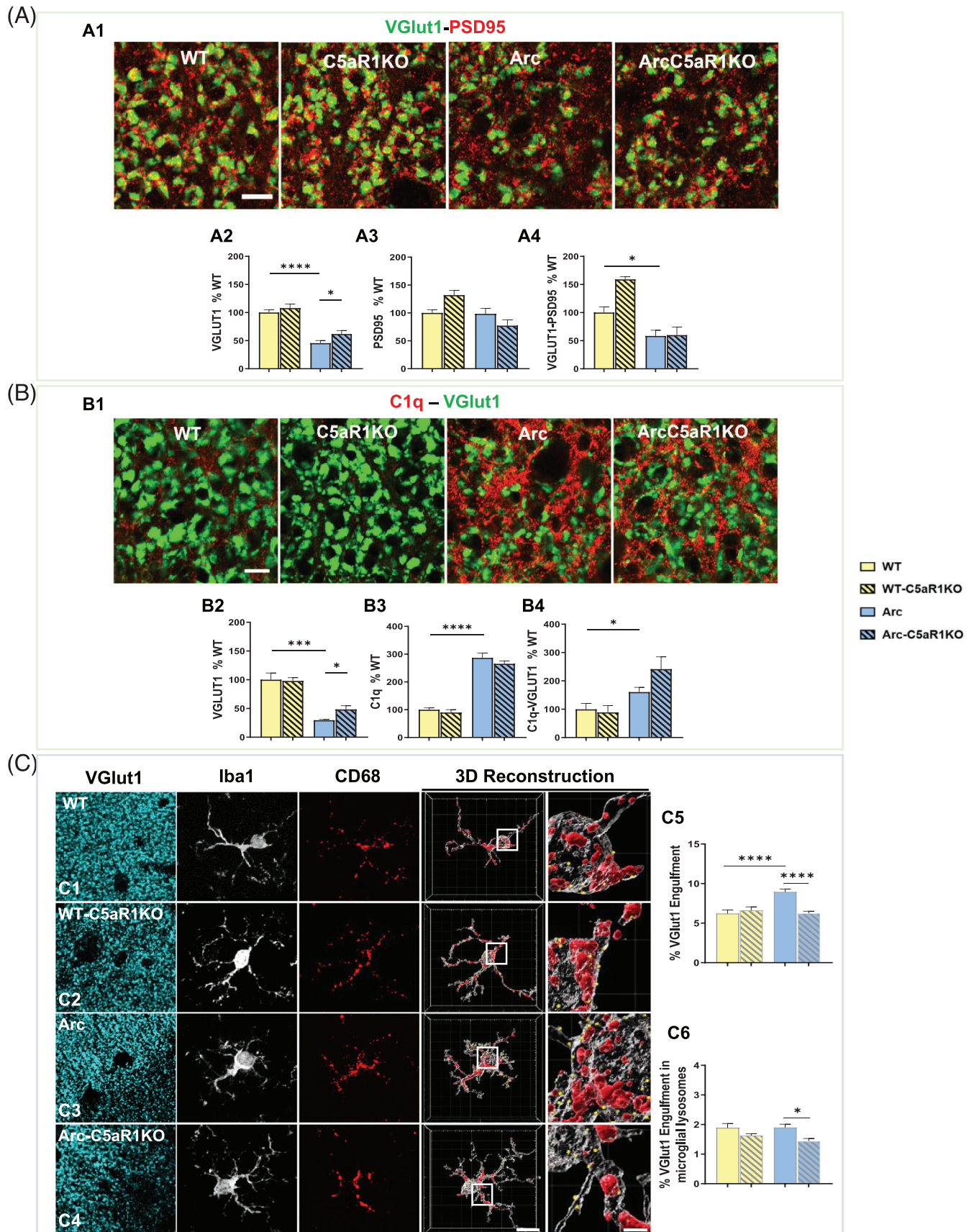


FIGURE 2 Lack of C5aR1 rescues VGLut1 presynaptic loss and reduces microglial engulfment despite higher C1q tagging in the CA3-SL hippocampal region at 10 months of age. A. Representative super-resolution images of VGLut1 (green) and PSD95 (red) synaptic puncta in the CA3-SL of 10 m Arc, Arc-C5aR1KO, and their respective WT littermates. Scale bar: 5 μ m (A1). Imaris quantitative analysis of VGLut1, PSD95, and

to determine if the absence of C5aR1 results in a reduced microglial phagocytosis of the synapses, we co-stained VGlut1 with the microglial markers Iba1 and CD68 (Figure 2C1-C4). Single microglial cells (and thus not plaque associated) in the CA3-SL region from all four genotypes were imaged and co-localization of presynaptic markers within the microglial cell body or within the microglial lysosomes were quantified using Imaris. Our results showed an increased amount of VGlut1 puncta within the microglial cell body in the Arctic mice (vs. WT), consistent with an increase in microglial phagocytosis of synapses. However, the absence of C5aR1 in the Arctic mouse model restored the VGlut1 engulfment down to WT levels (Figure 2C5), which mirrored the rescue of VGlut1 presynaptic density observed in the Arc-C5aR1KO mice (vs. Arctic) discussed above (Figure 2A2). This suggests that the excessive microglial engulfment observed in the Arctic mouse model of AD could be the main driver of the presynaptic loss described. No changes between WT and Arc mice were observed when the amount of VGlut1 puncta in the microglial lysosomes was analyzed, although a significant decrease was observed when comparing Arc-C5aR1KO versus Arctic mice (Figure 2C6), suggesting that microglial cells in the Arc-C5aR1KO mice might be more efficient in the degradation of the engulfed material in response to the severe amyloid pathology described in this AD model. Together, our results demonstrate a role of C5a-C5aR1 signaling in the excessive microglial presynaptic pruning that leads to synaptic loss and ultimately cognitive deficit at late stages of the pathology in the Arctic mouse model of AD.

3.3 | The beneficial effects of C5aR1 genetic ablation on the rescue of VGlut1 excessive presynaptic loss are dependent on the hippocampal region at 10 months of age

Since C5aR1 deletion reduced the loss of neuronal complexity at 10 months of age in both the CA1-SR²⁹ and CA3-SL (Supp Figure S3), we assessed the synaptic density in the CA1-SR region at 10 months of age (Figure 3A1-4), similarly to our analysis in the CA3-SL region described above. As expected at 10 months of age, a significant reduction in synaptic density was observed in the CA1-SR hippocampal region of Arc mice (compared to WT littermates) (Figure 3A4). However, in contrast to the CA3-SL region, while there was a significant and substantial decrease (41% reduction) in SP presynaptic puncta in Arctic mice (vs. WT), it was not rescued by deletion of C5aR1 (Arc-C5aR1KO vs. Arc mice) (Figure 3A2). As in our previous results in the CA3-SL, we did not observe any differences in the amount of PSD95

postsynaptic puncta among any of the genotypes at 10 months of age in the CA1-SR (Figure 3A3). SP-PSD95 colocalized puncta was significantly reduced in both Arc (49% reduction) and Arc-C5aR1KO (45% reduction) mice when compared to their control groups (Figure 3A4), suggesting that absence of C5aR1 did not have a significant effect in the CA1-SR hippocampal region. Similar results were observed when quantifying VGlut1 puncta and VGlut1-PSD95 colocalization in the same groups, age, and CA1-SR hippocampal region (data not shown). Similar to our previous results in the CA3-SL region, decreases were observed in both SP and VGlut1 presynaptic puncta in CA1-SR in the Arc and Arc-C5aR1KO mice that were accompanied by a significant increase in C1q deposition (Figure 3B-C) at the presynapses.

Double labelling of C3 and VGlut1 in the CA1-SR hippocampal region showed that while there were decreases in total SP or VGlut1 puncta in the Arc mice as seen in Figure 3B, 3C and Supp Figure S4B2, no significant differences in the total amount of C3 or C3 colocalized with VGlut1 were seen in any of the genotypes analyzed (Supp Figure S4B). Interestingly, in a different hippocampal region (DG-ML), no changes in synaptic puncta were observed across the different genotypes (Supp Figure S5A), despite the substantial increases in C1q and C1q tagged VGlut1 and SP synapses (Supp Figure S5B), further suggesting that changes in synaptic puncta are region specific and that C1q or iC3b tagging alone is not sufficient to trigger synaptic engulfment and synaptic loss.

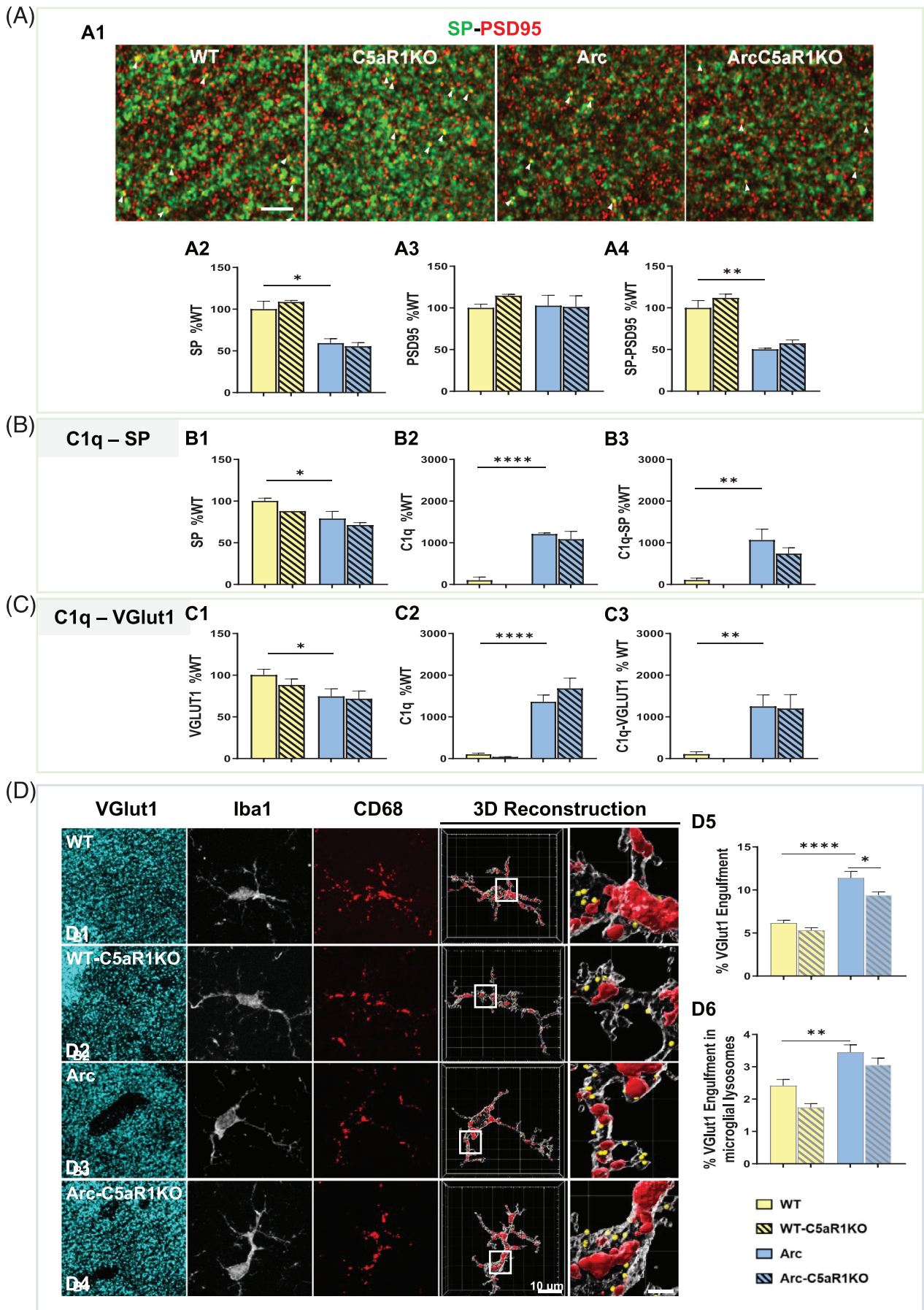
Analysis of VGlut1+ synapses engulfed by microglial cells in the CA1-SR region (Figure 3D) showed a significant reduction of VGlut1 puncta inside microglial cells in the absence of C5aR1 in the Arctic model (Arc-C5aR1KO), when compared to C5aR1 sufficient Arctic mice (Figure 3D5). These results suggest that, even if microglial synaptic pruning is reduced by C5aR1 deletion, this beneficial reduction is not enough to rescue the excessive presynaptic loss observed at 10 months of age in the Arctic model of AD in the CA1-SR region of the hippocampus.

Overall, our results demonstrated that C5a-C5aR1 signaling affects microglial synaptic engulfment and presynaptic loss in the Arctic mouse model of AD in a region dependent manner.

3.4 | C5a-C5aR1 influences synaptic loss and microglial synaptic engulfment in a region-specific dependent manner at 7 months of age

While behavioral deficits in the Arctic model were only observed at 10 months of age,²⁹ we investigated if synaptic loss and microglial

colocalized synaptic puncta (A2-A4). Data are shown as mean \pm SEM (normalized to WT control group) of 3-4 images per animal and 2-6 animals per genotype. B. Representative super-resolution images of C1q (red) and VGlut1 (green) synaptic puncta. Scale bar: 5 μ m (B1). Imaris quantification of C1q, VGlut1 and C1q-VGlut1 colocalization (B2-B4). Data are shown as mean \pm SEM (normalized to WT control group) of 3 images per animal and 4-5 animals per genotype. C. Confocal images and 3D reconstruction with surface rendering using Imaris software of individual microglial cells (Iba1+; grey), presynapses (VGlut1+; cyan), and lysosomes (CD68+; red). Scale bar: 10 μ m; inserts 2 μ m (C1-C4). Quantitative analysis of VGlut1+ presynaptic puncta engulfment per microglia (C5). Quantitative analysis of VGlut1+ presynaptic puncta localized within the microglial lysosomes (C6). Data are shown as mean \pm SEM of 15 individual microglial cells/mouse and $n = 3$ mice per genotype. * $p < 0.05$, *** $p < 0.001$, **** $p < 0.0001$ using one-way ANOVA (A-C) followed by Tukey's post hoc test and unpaired t-test (A).



synaptic pruning might precede cognitive deficit at an earlier stage of the disease (Figure 4A-C). Super-resolution microscopy (Figure 4A) showed a significant decrease in VGlut1 puncta (55% reduction) (Figure 4A1-A2), no changes in PSD95 (Figure 4A3) and a significant decrease in colocalized VGlut1-PSD95 puncta (47% reduction) (Figure 4A4) in the Arctic mice when compared to WT littermates at 7 months of age in the CA3-SL. Interestingly at this earlier age, Arc-C5aR1KO mice showed a trend for a partial rescue of this synaptic density (Figure 4A2, A4), when compared to Arctic mice. At this same age, the microglial engulfment of VGlut1 pre-synapses (Figure 4C) showed a significant increase in the Arctic genotype (vs. WT) with a trend for a reduction of VGlut1 puncta detected within the microglial cells in the Arc-C5aR1KO mice (Figure 4C5), thus correlating with the trend for an improvement in synaptic density observed in the Arc-C5aR1KO relative to the C5aR1 sufficient Arctic mice (Figure 4A2 and 4A4). No differences in the amount of VGlut1 puncta within the microglial lysosomes were found in any of the genotypes, suggesting that at 7 months of age, the lysosomal function is not affected by the amyloid pathology present in the Arc mouse model of AD (Figure 4C6). Furthermore, increased levels of C1q associated with VGlut1 presynaptic puncta were observed in the Arctic mice when compared to WT (Figure 4B), which correlates with the decrease in VGlut1 (Figure 4A2), colocalized VGlut1-PSD95 puncta (Figure 4A4) and VGlut1 microglial engulfment (Figure 4C5). However, since the amount of C1q puncta is the same in the Arc and Arc-C5aR1KO, changes in C1q tagging does not account for the partial rescue of the synaptic density (Figure 4A4) and synaptic engulfment observed in the absence of C5aR1 (Arc-C5aR1KO vs. Arc mice).

In contrast to what we observed at 7 months of age in the CA3-SL hippocampal region, no differences were found (Supp Figure S6) in VGlut1 presynaptic puncta (Supp Figure S6A1), PSD95 post-synaptic puncta (Supp Figure S6A2), VGlut1-PSD95 colocalized puncta (Supp Figure S6A3) or VGlut1 microglial engulfment (Supp Figure S6C) in any of the genotypes in the CA1-SR region at the same age, further supporting our previous results at 10 months of age where the role of C5a-C5aR1 in synaptic loss and synaptic engulfment is dependent upon the hippocampal region. In addition, we observed a significant increase in C1q tagged VGlut1 puncta (Supp Figure S6B2) in Arctic mice (compared to WT) in the CA1-SR hippocampal region at 7 months of age, which correlates with the increases in C1q-VGlut1 puncta that we observed at both 7 and 10 months of age in the CA1 and CA3 areas.

However, no differences were found in the total amount of VGlut1 presynaptic puncta engulfed by microglial cells (Supp Figure S6C5). These results further support our hypothesis that C1q tagging is not sufficient to drive the excessive hippocampal synaptic pruning and synaptic loss associated with AD.

Finally, we analyzed even earlier stages of the disease (2.7 and 5 months of age) to assess whether synaptic loss could precede the excessive accumulation of amyloid beta plaques observed in the Arctic model of AD. No changes in synaptic density (VGlut1-PSD95 colocalization) were observed among any of the genotypes at 2.7 (Supp Figure S7A) or 5 months of age (Supp Figure S7B) in any of the regions analyzed, suggesting that synaptic loss events occur at later stages of the disease, when amyloid plaques are dominant in the Arctic model.

3.5 | Pharmacological inhibition of C5aR1 rescues the excessive synaptic loss in the Tg2576 mouse model of AD

Besides the beneficial role of genetic ablation of C5aR1 in preventing the loss of neurite complexity, presynaptic loss (data reported in this manuscript) and cognitive deficits in the Arctic mouse model of AD,^{29,33} pharmacological inhibition of C5a-C5aR1 signaling with PMX205, a potent C5aR1 antagonist,^{31,32} in two different mouse models of AD has shown beneficial effects in modulating gene expression and preventing synaptic and cognitive deficits. Therefore, we analyzed synaptic density changes in the Tg2576 mouse model of AD upon PMX205 treatment (Supp Figure S1B). VGlut1 and PSD95 synaptic puncta were measured at 15 months of age in both the CA3-SL and CA1-SR hippocampal regions (Figure 5A-B). Our results in the CA3-SL area, showed a significant decrease (14% decrease) in VGlut1 presynaptic puncta (Figure 5A1-A2) and in VGlut1-PSD95 colocalized puncta (28% decrease) (Figure 5A4) in the Tg2576-H₂O mice (when compared to WT-H₂O) that was completely rescued when PMX205 was administered to Tg2576 (Tg2576-PMX205). Similar to our results in the Arctic model, no changes were observed in the PSD95 postsynaptic puncta density among any of the different groups (Figure 5A3). Interestingly, our previous results in the CA3-SL region showed an increase in the VGlut1 synaptic engulfment by microglial cells in the Tg2576-H₂O (vs. WT-H₂O) that was significantly reduced upon

FIGURE 3 Absence of C5aR1 in the Arctic model of AD fails to rescue presynaptic loss in the CA1-SR hippocampal region at 10 months of age. (A) Representative super-resolution images of SP (green) and PSD95 (red) at 10 months of age in CA1-SR (arrowheads show colocalization of pre and post synaptic puncta) Scale bar: 5 μ m. (A1). Quantitative analysis of SP, PSD95 and colocalized SP-PSD95 puncta (A2-A4). Data are shown as Mean \pm SEM (normalized to WT control group) of four to six images per animal and two to four animals per genotype. (B) Imaris quantification of SP, C1q, and C1q-SP colocalization from super-resolution images in CA1-SR. Data are shown as Mean \pm SEM (normalized to WT control group) of three images per animal and one to four mice per genotype. (C) Imaris quantification of VGlut1, C1q, and C1q-VGlut1 colocalization from super-resolution images in CA1-SR. Data are shown as Mean \pm SEM (normalized to WT control group) of three images per animal and three to seven mice per genotype. (D) Confocal images and 3D reconstruction with surface rendering using Imaris of individual microglial cells (Iba1+; grey), presynapses (VGlut1+; cyan), and lysosomes (CD68+; red). Scale bar: 10 μ m; inserts 2 μ m. (D1-D4). Quantitative analysis of VGlut1+ presynaptic puncta engulfment per microglia (D5). Quantitative analysis of VGlut1+ presynaptic puncta localized within the microglial lysosomes (D6). Data are shown as Mean \pm SEM of 15 individual microglial cells/mouse and $n = 3$ mice per genotype. * $p < 0.05$, ** $p < 0.01$, **** $p < 0.0001$ using one-way ANOVA (A-D) followed by Tukey's post hoc test.

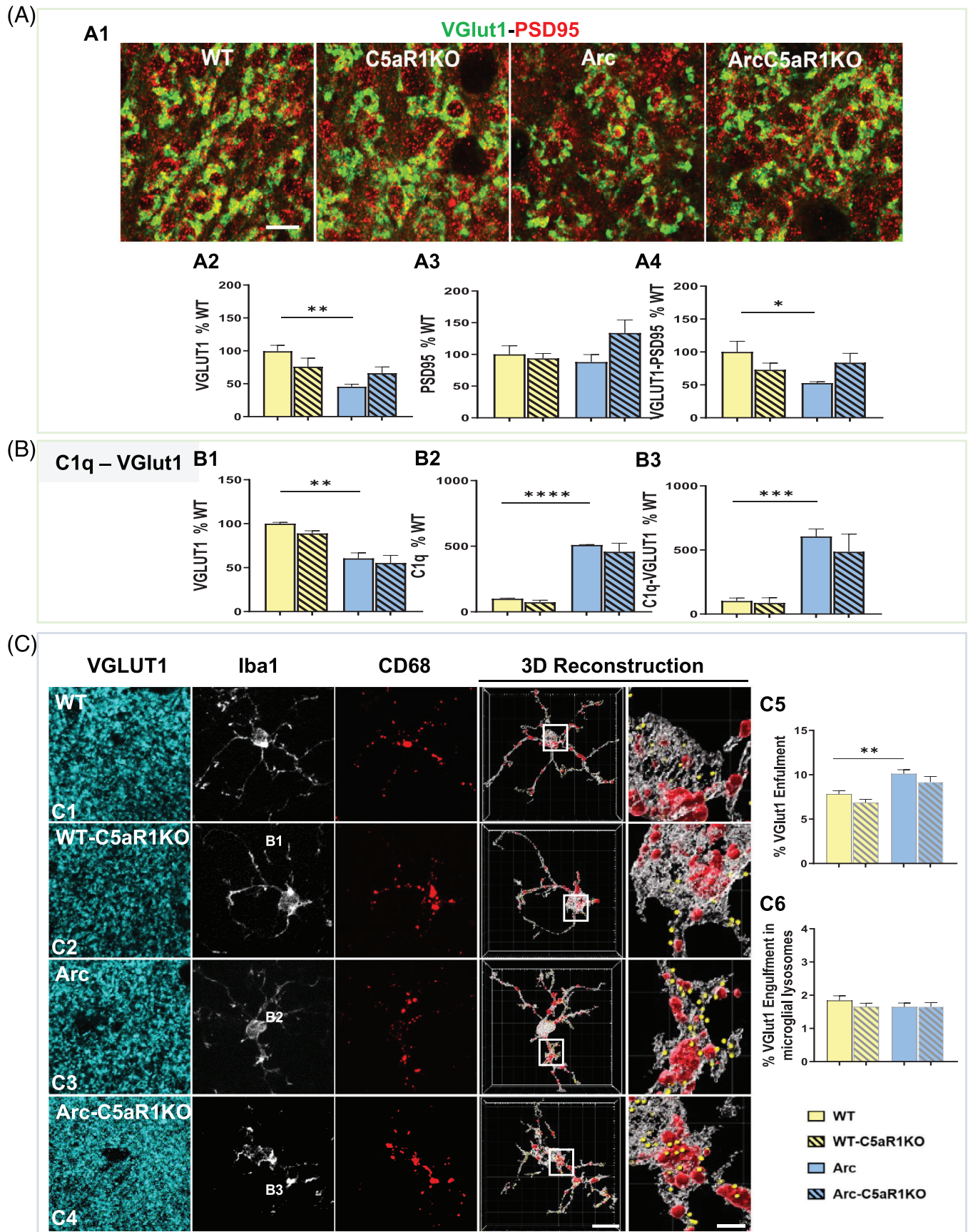


FIGURE 4 VGLut1 presynaptic loss in the Arctic mouse model of AD is not reversed in the absence of C5aR1 at 7 months in the CA3-SL region of the hippocampus. (A) Super-resolution representative images (A1) and quantitative analysis of VGLut1, PSD95, and colocalized VGLut1-PSD95

treatment with PMX205,³² together suggesting that C5aR1 antagonism reduces microglial synaptic pruning which results in the rescue of the excessive presynaptic loss and synaptic density observed in the Tg2576 mouse model of AD.

We next investigated synaptic changes in the CA1-SR region in the Tg2576 mice treated with PMX205 and our results showed again a significant decrease of VGlut1 presynaptic puncta (22% decrease) in the Tg2576-H₂O mice when compared to WT-H₂O littermates (Figure 5B1-B2). Treatment with PMX205 showed a trend towards the rescue of the excessive VGlut1 synaptic loss (Tg2576-PMX205 vs. Tg2576-H₂O; $p = 0.14$) and a significant increase in the PSD95 puncta in the Tg2576-PMX205 when compared to Tg2576-H₂O (Figure 5B3). Colocalized VGlut1-PSD95 puncta showed a significant decrease (37%) in the Tg2576-H₂O (vs. WT-H₂O) that (similar to the CA3-SL region) was rescued with PMX205 treatment (Figure 5B4). Interestingly, when single microglial cells in the CA1-SR region from all four groups were imaged and co-localization of VGlut1 within the microglial cell body or within the microglial lysosomes was quantified (Figure 5C1-C6), we observed a significant decrease in the amount of VGlut1+ presynaptic puncta within the microglial cell body in the Tg2576-H₂O mice (compared to WT-H₂O), suggesting that the loss of VGlut1 synapses observed in the CA1-SR region of the Tg2576 mouse model is not due to an excessive microglial synaptic pruning in this hippocampal region at this age (Figure 5C5). However, Tg2576-PMX205 treated mice did show reduced VGlut1 puncta localized within the microglial lysosomes (vs. Tg2576-H₂O mice) (Figure 5C6), consistent with our previous data in the Arctic model of AD and suggesting an improved lysosomal efficiency when C5aR1 signaling is suppressed. Overall, our results here demonstrated that pharmacological inhibition of C5a-C5aR1 signaling, by using a C5aR1 antagonist, can rescue the excessive synaptic loss observed in the Tg2576 mouse model of AD.

3.6 | Astrocytes contribute to excessive pre-synaptic loss only at late stages of the disease

It is well established that astrocytes as well as microglial cells can participate in synaptic pruning in the healthy and disease brain, playing a key role in the pruning of synapses and circuit remodeling.^{22,37} Therefore, we assessed if C5a-C5aR1 signaling could influence synaptic engulfment by astrocytes, applying our two different approaches, the genetic deletion of C5aR1 in the Arctic mouse model of AD (Supp Figure S1A) as well as the pharmacological inhibition of C5aR1 in the Tg2576 model of AD (Supp Figure S1B), where microglial ingestion of VGlut1 was not suppressed in CA1, while total VGlut1-PSD95

puncta was protected (Figure 5B-C). First, VGlut1 was co-stained with the astrocyte marker GFAP and the lysosomal marker Lamp2 and single astrocytes (and thus not plaque associated) were imaged at 10 and 7 months of age in the CA3-SL and the CA1-SR hippocampal region of WT, C5aR1KO, Arc, and Arc-C5aR1KO mice. At 10 months of age (Figure 6A) in the CA3-SL region, no difference was found in the VGlut1 puncta colocalized with GFAP+ astrocytic cell body in the Arctic mice versus the WT. However, Arc-C5aR1KO mice showed a significant reduction in the VGlut1 synaptic engulfment by astrocytes in the same age and region (vs. Arctic) (Figure 6A1). Importantly, colocalization of VGlut1 puncta within the astroglial lysosomes showed a significant increase in the Arc mice when compared to WT littermates, that was reduced back to WT levels by the absence of C5aR1 (Arc-C5aR1KO vs. Arc) (Figure 6A2), suggesting that, at least in the CA3-SL hippocampal region at this specific age, astrocytic synaptic pruning seems to be contributing to the excessive synaptic pruning, and that the absence of C5aR1 signaling suppresses this astrocyte engulfment of VGlut1. Similarly, at the same age (10 months) in the CA1-SR region, a significant reduction in the VGlut1 puncta located in the astroglial cell body was observed in the Arc-C5aR1KO versus Arc mice (Figure 6A3). Moreover, a significant increase in VGlut1+ puncta within the astroglial lysosomes (Arctic vs. WT) and a trend for a reduction in the engulfment when C5aR1 was ablated (Arc-C5aR1KO vs. Arc) was observed in the CA1-SR hippocampal region (Figure 6A4), which again, correlates with the excessive VGlut1 loss observed in the Arctic mice (Figure 3A2 and C1)). We then performed the same staining and quantification at 7 months of age (Figure 6B) in the same genotypes and our results showed a significant reduction of VGlut1 puncta colocalized with either the astrocyte cell body or the astroglial lysosomes in Arctic mice (when compared to WT controls) in the CA3-SL region (Figure 6B1-B2). In the CA1-SR area, we observed a significant reduction of VGlut1-GFAP colocalization in the Arc model (vs. WT) (Figure 6B3), but no change in astrocyte lysosomal VGlut1 (Figure 6B4). These results suggest that in contrast to microglia (Figure 4C5), astrocytes are not actively involved in excessive synaptic pruning and presynaptic loss observed in the Arctic mice at 7 months of age (Figure 4) and that C5aR1 deletion does not have an effect on astroglial synaptic engulfment at this stage in the Arctic model.

In contrast, the pharmacological inhibition of C5aR1 in Tg2576 and WT mice from 12-15 months of age, revealed no significant differences in the VGlut1 puncta localized in the astrocyte cell body in any of the experimental groups in the CA3-SL region (Figure 6C1), while a significant reduction in the lysosomal VGlut1+ puncta was observed in the Tg2576-PMX205 mice when compared to the Tg2576-H₂O control group (Figure 6C2), suggesting that lack of C5aR1 signaling might

puncta (A2-A4) in CA3-SL of 7 m WT, WT-C5aR1KO, Arc, and Arc-C5aR1KO. Scale bar: 5 μ m. Data are shown as mean \pm SEM (normalized to WT control group) of three images per animal and $n = 3-4$ per genotype. (B) Quantitative analysis of VGlut1, C1q and C1q-VGlut1 colocalized puncta in CA3-SL at 7 months of age. Data are shown as mean \pm SEM (normalized to WT control group) of three images per animal and $n = 3-4$ per genotype. (C) Confocal images and 3D reconstruction of Iba1, CD68 and VGlut1 in CA3-SL at 7 months of age in the Arctic mouse model of AD. Scale bar: 10 μ m; inserts 2 μ m (C1-C4). Quantitative analysis of VGlut1+ presynaptic puncta engulfment per microglia (C5). Quantitative analysis of VGlut1+ presynaptic puncta localized within the microglial lysosomes (C6). Data are shown as mean \pm SEM of 15 individual microglial cells/mouse and $n = 3-4$ mice per genotype. * $p < 0.05$, ** $p < 0.01$, *** $p < 0.001$, **** $p < 0.0001$ using one-way ANOVA (A-C) followed by Tukey's post hoc test.

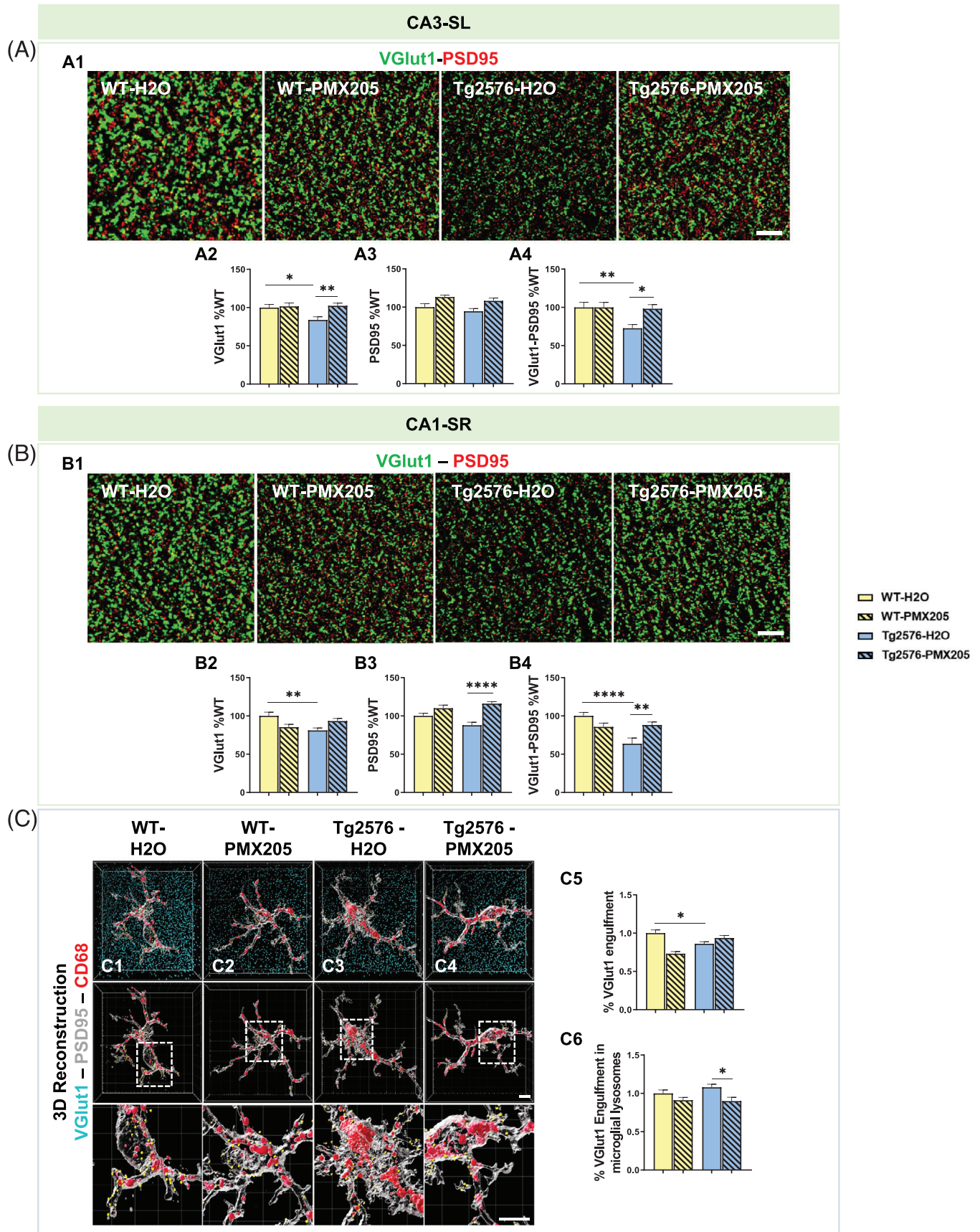


FIGURE 5 Treatment with PMX205 rescues the excessive synaptic loss observed in the Tg2576 mouse model of AD. (A-B) Representative super-resolution images of VGlut1 (green) and PSD95 (red) puncta in the CA3-SL (A1) or CA1-SR (B1) hippocampal region of 15 months old WT

enable increased lysosomal degradation activity. In the CA1-SR, we observed a reduction in VGlut1 engulfment by astrocytes (Tg2576-H₂O vs. WT-H₂O) as well as the VGlut1+ puncta located in the astroglial lysosomes, which was further reduced by treatment with PMX205 (Tg2576-PMX205 vs. Tg2576-H₂O), similar to our observations in the CA3-SL region (Figure 6C3-C4). These results suggest that astrocyte lysosomal activity is influenced as a result of C5a-C5aR1 signaling, but that astrocytes have a very limited role in synaptic elimination in the less aggressive amyloidogenic Tg2576 mouse models. Astrocyte contribution to the excessive synaptic pruning and synaptic loss were only seen at late stages (10 mo of age) of the disease in the aggressive Arctic48 mouse model of AD.

4 | DISCUSSION

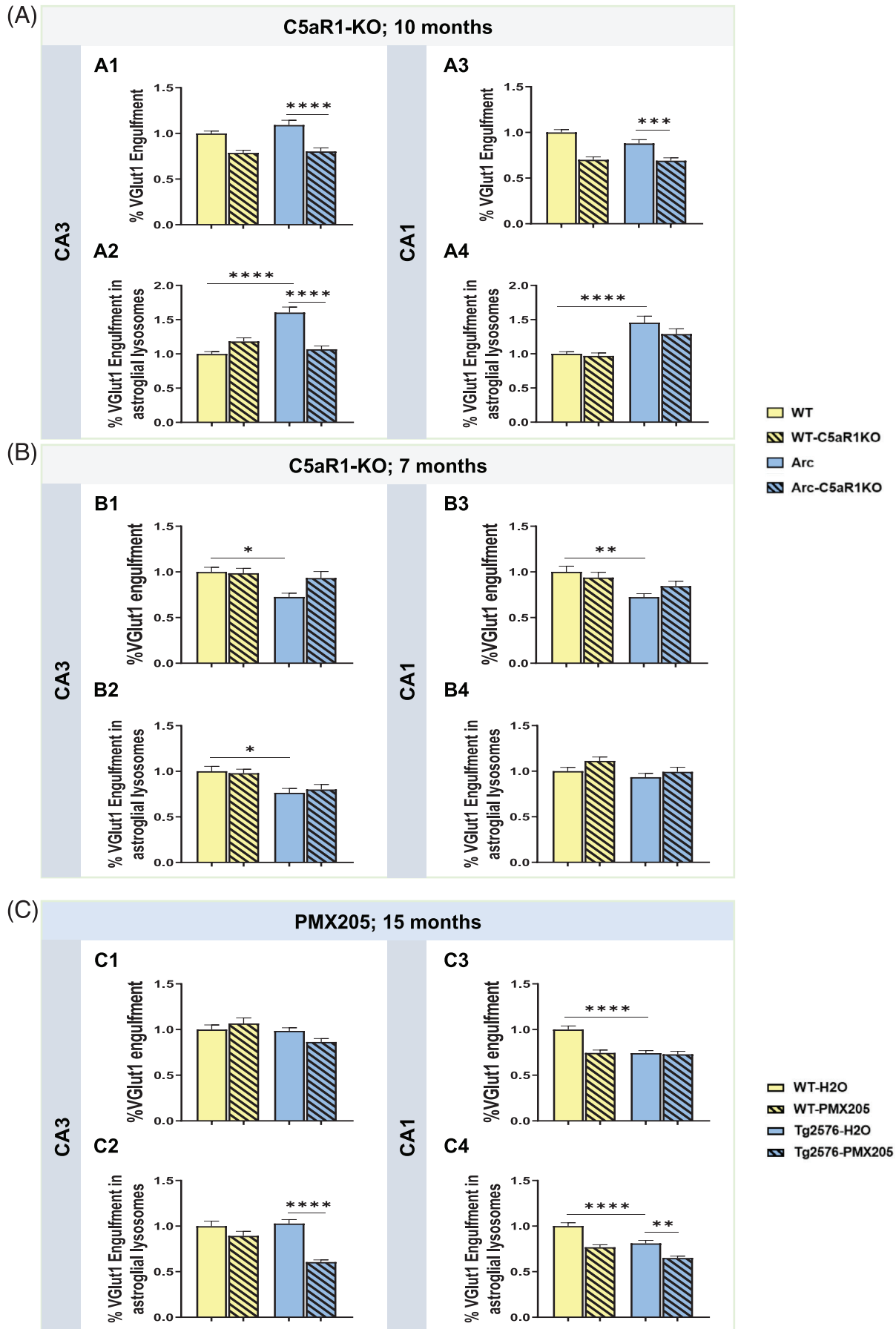
Synaptic loss is the strongest correlate for cognitive impairment in AD^{20,44} and recent GWAS studies uncovered multiple AD risk variants that converge on phagocytic pathways in microglial cells.⁴⁵ Avoiding excess synaptic pruning that leads to cognitive impairment in AD and other related disorders could have substantial impact on the lives of individuals with the disease and their caregivers. Preclinical studies in mouse models of AD are essential for the development of potential therapeutics. Indeed, complement activation has been shown to cause aberrant synapse pruning in mouse models of AD and other neurodegenerative disorders.^{18,22,46} Deletion of C1q, C3, and C4 reduce the excessive synaptic loss described in multiple models of neurodegenerative disorders.^{23,26,47} However, the deletion of those upstream components of the complement cascade also suppresses the generation of C5a and, thus, does not distinguish the potential contribution of C5a-C5aR1 signaling on synaptic pruning. Here, the role of C5a-C5aR1 interaction on synaptic pruning was investigated using the Arctic48 model of AD in which C5aR1 was genetically ablated, as well as the Tg2576 model of AD treated with a C5aR1 antagonist (PMX205). In the more aggressive Arctic model, there is an age and region-specific contribution of C5aR1 on synaptic pruning, as the deletion of this receptor results in reduced synaptic engulfment by microglia and a partial restoration of synaptic density in the CA3-SL at 7 (Figure 4) and 10 months (Figure 2) of age. In addition, pharmacological inhibition of C5aR1 in the Tg2576 model of AD also rescued the excessive synaptic loss observed in this mouse model at 15 months of age in both CA3 and CA1 (Figure 5). These results are consistent with both the rescue of LTP (Figure 1) and of neuronal integrity in the Arc-C5aR1KO mice (Supp Figure S3 and²⁹), as well as the cognitive protection observed previously with C5aR1 antagonist treatment of Tg2576 mice and the

C5aR1 deficient Arctic model of AD^{29,31} and a role for C5aR1 signaling in oligomeric A β enhancement of LTD.⁴⁸

Synaptic pruning has been shown to occur by microglial engulfment through the CR3 receptor²¹; however, the exact mechanism is still unclear. Recent work indicates that trogocytosis of presynaptic elements in a CR3-independent manner may also be involved.⁴⁹ Synaptic pathology in AD has been associated to alterations in both the pre-synaptic and post-synaptic terminals⁵⁰; however, a meta-analysis covering more than 400 publications⁵¹ as well as an in-depth proteomics study pointed to a presynaptic failure in AD patients.⁵² We have observed an age- and region-specific substantial loss of presynaptic markers in the Arctic and Tg2576 models of AD (Figures 2–5), that correlated with higher VGlut1 engulfment by microglial cells. Genetic ablation or pharmacological inhibition of C5aR1 partially rescues the excessive microglial synaptic pruning and restores synaptic density in the CA3-SL, suggesting that microglial phagocytic capacity for presynaptic puncta could be a main driver involved in the synaptic density changes observed here. It is known that C5a-C5aR1 interaction on microglial cells produces a more inflammatory environment and suppresses clearance pathways both of which could contribute to neuronal damage and cognitive impairment.²⁹ Furthermore, the downregulation of a microglial cluster involved in synaptic pruning in Tg2576 mice treated with a C5aR1 antagonist³² could contribute to the results presented here. Nevertheless, the possibility that C5a-C5aR1 signaling could also directly impact neurons cannot be ruled out. Functional C5aR1 expression has been shown in primary rodent cell cultures,^{53,54} in mouse cortical neurons,⁵⁵ and in the SL⁵⁶ where the mossy fibers coming from the granule cells of the DG contact pyramidal neurons of the hippocampal CA3 area. This pathway is involved in spatial memory formation and consolidation of hippocampal dependent memory,⁵⁷ suggesting that the presence of C5aR1 in the presynaptic terminals of the mossy fibers would enable a neuromodulatory role for C5a-C5aR1 signaling. Indeed, it is precisely in the CA3-SL region where we observed the preservation of pre-synaptic density when the C5a-C5aR1 axis is impaired (Figure 2).

Levels of C1q increase with age and disease in several mouse models and in human AD brain.^{9,41} We have previously shown that C1q is locally synthesized by microglia and is significantly increased in the Arctic model of AD.⁴⁰ In addition, it was reported that C1q tags synapses in several AD and tauopathy mouse models^{23,58} and that it preferentially tags the presynaptic portion, which can be directly linked to apoptotic changes in the synapse.⁵⁹ In line with this, here we showed a significant increase in C1q tagging of presynapses at 7 and 10 months of age in Arctic mice. Whether C1q associates with just “weak” synapses is not clear, as, stronger/more active synapses could be

and Tg2576 treated with either vehicle (H₂O) or PMX205. Scale bar: 5 μ m. Quantitative analysis of VGlut1, PSD95, and colocalized synaptic puncta in the CA3-SL (A2-A4) or CA1-SR (B2-B4). Data are shown as mean \pm SEM (normalized to WT control group) of 3–4 images per mouse and $n = 4–5$ mice per group. (C) Imaris 3D reconstruction with surface rendering of individual microglial cells (Iba1+; grey), presynapses (VGlut1+; cyan), and lysosomes (CD68+; red). Scale bar: C1-C4: 5 μ m; inserts 2 μ m (C1-C4). Quantitative analysis of VGlut1+ presynaptic puncta engulfment per microglia (C5). Quantitative analysis of VGlut1+ presynaptic puncta localized within the microglial lysosomes (C6). Data are shown as Mean \pm SEM of 15 individual microglial cells/mouse and $n = 4–5$ mice per group. * $p < 0.05$, ** $p < 0.01$, **** $p < 0.0001$ using two-way ANOVA (A–B) followed by Tukey's post hoc test.



protected by complement regulatory proteins or by activity dependent factors.^{46,60} However, from our data (Figures 2–4 and Supp Figure S5), it is clear that C1q association with presynaptic markers is not sufficient for engulfment to occur as the amount of C1q bound to synapses did not necessarily correlate with the changes observed in microglial synaptic engulfment or synaptic density in the Arctic model of AD (Figures 2 – 4). Additionally, C3 presynaptic deposition did not correlate with the extent of synaptic pruning (Supp Figure S4). Thus, while C1q, complement activation and CR3 are critical in excessive synaptic pruning in AD models, changes in microglia engulfment capacity, including those induced by C5a-C5aR1 signaling contribute to synaptic survival. As mentioned above, differential gene expression data in Arctic mice lacking C5aR1³³ are consistent with such a mechanism.

In addition to microglial cells, astrocytes have a vital role in synapse formation and maintenance and can also eliminate synapses during development and also in adulthood.^{36,61} Moreover, astrocytes preferentially eliminate excitatory synapses in a C1q-dependent manner in the Tau P301S tauopathy mouse model and can compensate for microglial dysfunction by increasing their engulfment of inhibitory synapses around amyloid plaques in the TauPS2APP;Trem2^{KO} model.³⁷ Here, we demonstrated a role for astrocytes in excitatory (VGlut1+) synaptic engulfment at late stages of the pathology in the Arctic48 model of AD, and importantly, showed that genetic ablation of C5aR1 reduces synaptic pruning by astrocytes (Figure 6). We did not observe a significant contribution from astrocytes in the excessive presynaptic pruning at earlier stages of the disease in the Arctic model or in the less aggressive Tg2576 model. Whether this is due to astrocytes not being appropriately activated at earlier stages of pathology with less amyloid deposition or to insufficient signaling from microglia to astrocytes to upregulate phagocytic pathways remains to be determined.

Others have previously shown C1q-independent but C3-dependent synapse pruning processes,⁴³ as well as complement independent synapse elimination,¹⁸ which is a logical extension from humans and models genetically lacking C1q or C3. Stephan and colleagues showed significant increases in C1q in adult mice with no associated synaptic loss, but with a circuitry reorganization, suggesting that C1q may also act independently of the complement cascade,⁴¹ as was also reported in mouse retina during development.⁶² This could be the result of differential synthesis of complement components in response to increasing challenge or disease progression (reviewed in ref.³). Whether TREM2 also plays a role in the excessive pre-synaptic elimi-

nation that we showed here or whether, other “eat-me”, “don’t eat-me”, and/or complement regulatory molecules (CD47, SIRP α , CSMD1/2, neuronal pentraxins)^{63–67} are involved are yet to be determined and will likely direct future therapeutic targets. It will also be intriguing to determine if C1q at the high levels seen in AD would interfere with the action of several C1q-like molecules expressed in the nervous system that play roles in synapse formation and function.^{68,69}

In summary, the absence of C5aR1 (either by genetic ablation or by pharmacological inhibition) partially averts the excessive microglial synaptic pruning and presynaptic loss in two mouse models of AD and prevents LTP deficits, consistent with a significant role for C5a-C5aR1 signaling in these pathological events. Regardless of which (or all) of the mechanisms discussed above are involved in these processes, specifically targeting C5a-C5aR1 signaling could both reduce the excessive synaptic pruning of “stressed-but-viable”⁷⁰ neuronal synapses and suppress neurotoxic inflammation, without suppressing the protective functions of the complement system and other innate immune systems both in the central nervous system (CNS) and in the periphery. Importantly, avacopan, a small molecule C5aR1 antagonist,^{34,71} has recently been granted Food and Drug Administration (FDA) approval for a peripheral inflammatory disorder. Furthermore, PMX53, similar to PMX205, was shown to be safe in a small phase 1b trial.⁷² Thus, precision targeting of C5aR1 is a promising novel therapeutic candidate for prevention and treatment of AD. Combining C5aR1 targeted therapy with strategies targeting other aspects of AD pathology may be even more effective for the various subtypes seen in clinical cases of AD.

ACKNOWLEDGEMENTS

We thank Enrico Gratton and Rachel Cinco in the Laboratory for Fluorescence Dynamics, Department of Biomedical Engineering University of California, Irvine, CA for their help and use of the Airyscan. This study was made possible in part through access to the Optical Biology Core Facility of the Developmental Biology Center, a shared resource supported by the Cancer Center Support Grant (CA-62203) and Center for Complex Biological Systems Support Grant (GM-076516) at the University of California, Irvine. Work was supported by NIH R01 AG060148, R21 AG061746 (AJT), R01 AG076835 (MAW) and U54 AG054349, Larry L. Hillblom postdoctoral fellowship #2021-A-020-FEL (AGA), Alzheimer’s Association Research Fellowship AARFD-20-677771 (NDS), and the Edythe M. Laudati Memorial Fund (AJT).

FIGURE 6 Contribution to VGlut1 synaptic engulfment by astrocytes differs based on age, region, and the AD mouse model analyzed. (A) Quantitative analysis of VGlut1+ presynaptic puncta engulfed per astrocyte (A1, A3) or localized within the astroglial lysosomes (A2, A4) at 10 months of age in WT, WT-C5aR1KO, Arc, and Arc-C5aR1KO mice. Data are shown as mean \pm SEM (normalized to WT control group) of 15 individual astroglial cells/mouse and $n = 4$ mice per genotype. (B) Quantitative analysis of VGlut1+ presynaptic puncta engulfed per astrocyte (B1, B3) or VGlut1+ presynaptic puncta localized within the astroglial lysosomes (B2, B4) at 7 months of age in WT, WT-C5aR1KO, Arc, and Arc-C5aR1KO mice. Data are shown as Mean \pm SEM (normalized to WT control group) of 15 individual astroglial cells/mouse and $n = 3-4$ mice per genotype. (C) Quantitative analysis of VGlut1+ presynaptic puncta engulfed per astrocyte (C1, C3) or VGlut1+ presynaptic puncta localized within the astroglial lysosomes at 15 months of age in WT-H₂O, WT-PMX205, Tg2576-H₂O and Tg2576-PMX205 mice (C2, C4). Data are shown as mean \pm SEM (normalized to WT-H₂O control group) of 15 individual astroglial cells/mouse and $n = 4-5$ mice per genotype. * $p < 0.05$, ** $p < 0.01$, *** $p < 0.001$, **** $p < 0.0001$ using two-way ANOVA (A-C) followed by Tukey’s post hoc test.

CONFLICTS OF INTEREST STATEMENT

The authors declare no conflicts of interest. Author disclosures are available in the supporting information.

CONSENT STATEMENT

No human subjects were used for the present study. Therefore, consent was not necessary.

ORCID

Andrea J. Tenner  <https://orcid.org/0000-0003-3000-024X>

REFERENCES

1. Querfurth HW, LaFerla FM. Alzheimer's disease. *N Engl J Med*. 2010;362(4):329-344.
2. Akiyama H, Barger S, Barnum S, et al. Inflammation and Alzheimer's disease. *Neurobiol Aging*. 2000;21(3):383-421.
3. Bohlsion SS, Tenner AJ. Complement in the brain: contributions to neuroprotection, neuronal plasticity, and neuroinflammation. *Annu Rev Immunol*. 2023;41:431-452.
4. Carpanini SM, Harwood JC, Baker E, et al. The impact of complement genes on the risk of late-onset Alzheimer's disease. *Genes (Basel)*. 2021;12(3):443.
5. Rogers J, Cooper NR, Webster S, et al. Complement activation by beta-amyloid in Alzheimer disease. *Proc Natl Acad Sci*. 1992;89:10016-10020.
6. Shen Y, Lue L, Yang L, et al. Complement activation by neurofibrillary tangles in Alzheimer's disease. *Neuroscience Letters*. 2001;305(3):165-168.
7. Cribbs DH, Velazquez P, Soreghan B, Glabe CG, Tenner AJ. Complement activation by cross-linked truncated and chimeric full-length beta-amyloid. *NeuroReport*. 1997;8(16):3457-3462.
8. Zhou J, Fonseca MI, Pisalyaput K, Tenner AJ. Complement C3 and C4 expression in C1q sufficient and deficient mouse models of Alzheimer's disease. *J Neurochem*. 2008;106(5):2080-2092.
9. Fonseca MI, Chu SH, Berci AM, et al. Contribution of complement activation pathways to neuropathology differs among mouse models of Alzheimer's disease. *J Neuroinflammation*. 2011;8(1):4.
10. Afagh A, Cummings BJ, Cribbs DH, Cotman CW, Tenner AJ. Localization and cell association of C1q in Alzheimer's disease brain. *Exp Neurol*. 1996;138(1):22-32.
11. Veerhuis R, Janssen I, Hack CE, Eikelenboom P. Early complement components in Alzheimer's disease brains. *Acta Neuropathologica*. 1996;91(1):53-60.
12. Morgan BP. Complement in the pathogenesis of Alzheimer's disease. *Semin Immunopathol*. 2018;40(1):113-124.
13. Wu T, Dejanovic B, Gandham VD, et al. Complement C3 is activated in human AD brain and is required for neurodegeneration in mouse models of amyloidosis and tauopathy. *Cell Rep*. 2019;28(8):2111-2123.e6.
14. Zhang B, Gaiteri C, Bodea LG, et al. Integrated systems approach identifies genetic nodes and networks in late-onset Alzheimer's disease. *Cell*. 2013;153(3):707-720.
15. Schartz ND, Tenner AJ. The good, the bad, and the opportunities of the complement system in neurodegenerative disease. *J Neuroinflammation*. 2020;17(1):354.
16. Ager RR, Fonseca MI, Chu SH, et al. Microglial C5aR (CD88) expression correlates with amyloid-beta deposition in murine models of Alzheimer's disease. *J Neurochem*. 2010;113(2):389-401.
17. Woodruff TM, Ager RR, Tenner AJ, Noakes PG, Taylor SM. The role of the complement system and the activation fragment C5a in the central nervous system. *Neuromolecular Med*. 2009;12(2):179-192.
18. Stevens B, Allen NJ, Vazquez LE, et al. The classical complement cascade mediates CNS synapse elimination. *Cell*. 2007;131(6):1164-1178.
19. Parker SE, Bellingham MC, Woodruff TM. Complement drives circuit modulation in the adult brain. *Prog Neurobiol*. 2022;214:102282.
20. Selkoe DJ. Alzheimer's disease is a synaptic failure. *Science*. 2002;298(5594):789-791.
21. Schafer DP, Lehrman EK, Kautzman AG, et al. Microglia sculpt postnatal neural circuits in an activity and complement-dependent manner. *Neuron*. 2012;74(4):691-705.
22. Gomez-Arboledas A, Acharya MM, Tenner AJ. The role of complement in synaptic pruning and neurodegeneration. *Immunotargets Ther*. 2021;10:373-386.
23. Hong S, Beja-Glasser VF, Nfonoyim BM, et al. Complement and microglia mediate early synapse loss in Alzheimer mouse models. *Science*. 2016;352(6286):712-716.
24. Sokolova D, Childs T, Hong S. Insight into the role of phosphatidylinositol in complement-mediated synapse loss in Alzheimer's disease. *Fac Rev*. 2021;10:19.
25. Kovacs RA, Vadaszi H, Bulyaki E, et al. Identification of neuronal pentraxins as synaptic binding partners of C1q and the involvement of NP1 in synaptic pruning in adult mice. *Front Immunol*. 2020;11:599771.
26. Sekar A, Bialas AR, de Rivera H, et al. Schizophrenia risk from complex variation of complement component 4. *Nature*. 2016;530(7589):177-183.
27. Benoit ME, Hernandez MX, Dinh ML, Benavente F, Vasquez O, Tenner AJ. C1q-induced LRP1B and GPR6 proteins expressed early in Alzheimer disease mouse models, are essential for the C1q-mediated protection against amyloid-beta neurotoxicity. *J Biol Chem*. 2013;288(1):654-665.
28. Petrisko TJ, Gomez-Arboledas A, Tenner AJ. Complement as a powerful "influencer" in the brain during development, adulthood and neurological disorders. *Adv Immunol*. 2021;152:157-222.
29. Hernandez MX, Jiang S, Cole TA, et al. Prevention of C5aR1 signaling delays microglial inflammatory polarization, favors clearance pathways and suppresses cognitive loss. *Mol Neurodegener*. 2017;12(1):66.
30. Landlinger C, Oberleitner L, Gruber P, et al. Active immunization against complement factor C5a: a new therapeutic approach for Alzheimer's disease. *J Neuroinflammation*. 2015;12:150.
31. Fonseca MI, Ager RR, Chu SH, et al. Treatment with a C5aR antagonist decreases pathology and enhances behavioral performance in murine models of Alzheimer's disease. *J Immunol*. 2009;183(2):1375-1383.
32. Gomez-Arboledas A, Carvalho K, Balderrama-Gutierrez G, et al. C5aR1 antagonism alters microglial polarization and mitigates disease progression in a mouse model of Alzheimer's disease. *Acta Neuropathol Commun*. 2022;10(1):116.
33. Carvalho K, Schartz ND, Balderrama-Gutierrez G, et al. Modulation of C5a-C5aR1 signaling alters the dynamics of AD progression. *J Neuroinflammation*. 2022;19(1):178.
34. Jayne DRW, Merkel PA, Schall TJ, Bekker P, Group AS. Avacopan for the Treatment of ANCA-Associated Vasculitis. *N Engl J Med*. 2021;384(7):599-609.
35. Woodruff TM, Nandakumar KS, Tedesco F. Inhibiting the C5-C5a receptor axis. *Mol Immunol*. 2011;48(14):1631-1642.
36. Lee JH, Kim JY, Noh S, et al. Astrocytes phagocytose adult hippocampal synapses for circuit homeostasis. *Nature*. 2021;590(7847):612-617.
37. Dejanovic B, Wu T, Tsai MC, et al. Complement C1q-dependent excitatory and inhibitory synapse elimination by astrocytes and microglia in Alzheimer's disease mouse models. *Nat Aging*. 2022;2(9):837-850.
38. Cheng IH, Palop JJ, Esposito LA, Bien-Ly N, Yan F, Mucke L. Aggressive amyloidosis in mice expressing human amyloid peptides with the Arctic mutation. *Nat Med*. 2004;10(11):1190-1192.
39. Hsiao KK, Chapman P, Nilsen S, et al. Correlative memory deficits, A β elevations, and amyloid plaques in transgenic mice. *Science*. 1996;274:99-102.

40. Fonseca MI, Chu SH, Hernandez MX, et al. Cell-specific deletion of C1q identifies microglia as the dominant source of C1q in mouse brain. *J Neuroinflammation*. 2017;14(1):48.
41. Stephan AH, Madison DV, Mateos JM, et al. A dramatic increase of C1q protein in the CNS during normal aging. *J Neurosci*. 2013;33(33):13460-13474.
42. Barthet G, Mulle C. Presynaptic failure in Alzheimer's disease. *Prog Neurobiol*. 2020;194:101801.
43. Werneburg S, Jung J, Kunjamma RB, et al. Targeted complement inhibition at synapses prevents microglial synaptic engulfment and synapse loss in demyelinating disease. *Immunity*. 2020;52(1):167-182. e7.
44. Mecca AP, O'Dell RS, Sharp ES, et al. Synaptic density and cognitive performance in Alzheimer's disease: a PET imaging study with [(11)C]UCB-J. *Alzheimers Dement*. 2022;18(12):2527-2536.
45. Podlesny-Drabiniok A, Marcora E, Goate AM. Microglial phagocytosis: a disease-associated process emerging from Alzheimer's disease genetics. *Trends Neurosci*. 2020;43(12):965-979.
46. Stephan AH, Barres BA, Stevens B. The complement system: an unexpected role in synaptic pruning during development and disease. *Annu Rev Neurosci*. 2012;35:369-389.
47. Shi Q, Chowdhury S, Ma R, et al. Complement C3 deficiency protects against neurodegeneration in aged plaque-rich APP/PS1 mice. *Sci Transl Med*. 2017;9(392):eaaf6295.
48. Ng AN, Salter EW, Georgious J, Bortolotto ZA, Collingridge GL. Amyloid- β 1-42 oligomers enhance mGlu5R-dependent synaptic weakening via NMDAR activation and complement C5aR1 signaling. *iScience*. 2023;26(12):108412.
49. Weinhard L, di Bartolomei G, Bolasco G, et al. Microglia remodel synapses by presynaptic trogocytosis and spine head filopodia induction. *Nat Commun*. 2018;9(1):1228.
50. Griffiths J, Grant SGN. Synapse pathology in Alzheimer's disease. *Semin Cell Dev Biol*. 2023;139:13-23.
51. de Wilde MC, Overk CR, Sijben JW, Masliah E. Meta-analysis of synaptic pathology in Alzheimer's disease reveals selective molecular vesicular machinery vulnerability. *Alzheimers Dement*. 2016;12(6):633-644.
52. Haytural H, Mermelekas G, Emre C, et al. The proteome of the dentate terminal zone of the perforant path indicates presynaptic impairment in Alzheimer disease. *Mol Cell Proteomics*. 2020;19(1):128-141.
53. Hernandez MX, Namirani P, Nguyen E, Fonseca MI, Tenner AJ. C5a increases the injury to primary neurons elicited by fibrillar amyloid beta. *ASN Neuro*. 2017;9(1):1759091416687871.
54. O'Barr SA, Caguioa J, Gruol D, et al. Neuronal expression of a functional receptor for the C5a complement activation fragment. *J Immunol*. 2001;166(6):4154-4162.
55. Pavlovski D, Thundiyil J, Monk PN, Wetsel RA, Taylor SM, Woodruff TM. Generation of complement component C5a by ischemic neurons promotes neuronal apoptosis. *FASEB J*. 2012;26(9):3680-3690.
56. Crane JW, Baiquni GP, Sullivan RK, et al. The C5a anaphylatoxin receptor CD88 is expressed in presynaptic terminals of hippocampal mossy fibres. *J Neuroinflammation*. 2009;6:34.
57. Ramirez-Amaya V, Balderas I, Sandoval J, Escobar ML, Bermudez-Rattoni F. Spatial long-term memory is related to mossy fiber synaptogenesis. *J Neurosci*. 2001;21(18):7340-7348.
58. Dejanovic B, Huntley MA, De Maziere A, et al. Changes in the synaptic proteome in tauopathy and rescue of tau-induced synapse loss by C1q antibodies. *Neuron*. 2018;100(6):1322-1336. e7.
59. Gyorffy BA, Kun J, Torok G, et al. Local apoptotic-like mechanisms underlie complement-mediated synaptic pruning. *Proc Natl Acad Sci U S A*. 2018;115(24):6303-6308.
60. Zhou J, Wade SD, Graykowski D, et al. The neuronal pentraxin Nptx2 regulates complement activity and restrains microglia-mediated synapse loss in neurodegeneration. *Sci Transl Med*. 2023;15(689):eadf0141.
61. Chung WS, Clarke LE, Wang GX, et al. Astrocytes mediate synapse elimination through MEGF10 and MERTK pathways. *Nature*. 2013;504(7480):394-400.
62. Burger CA, Jiang D, Li F, Samuel MA. C1q regulates horizontal cell neurite confinement in the outer retina. *Front Neural Circuits*. 2020;14:583391.
63. Lehrman EK, Wilton DK, Litvina EY, et al. CD47 protects synapses from excess microglia-mediated pruning during development. *Neuron*. 2018;100(1):120-134. e6.
64. Jiang D, Burger CA, Akhanov V, et al. Neuronal signal-regulatory protein alpha drives microglial phagocytosis by limiting microglial interaction with CD47 in the retina. *Immunity*. 2022;55(12):2318-2335. e7.
65. Kovács RÁ, Vadász H, Bulyáki É, et al. Identification of neuronal pentraxins as synaptic binding partners of C1q and the involvement of NP1 in synaptic pruning in adult mice. *Front Immunol*. 2021;11(3792):599771.
66. Rueda-Carrasco J, Sokolova D, Lee SE, et al. Microglia-synapse engulfment via PtdSer-TREM2 ameliorates neuronal hyperactivity in Alzheimer's disease models. *EMBO J*. 2023;42(19):e113246.
67. Zhong L, Sheng X, Wang W, et al. TREM2 receptor protects against complement-mediated synaptic loss by binding to complement C1q during neurodegeneration. *Immunity*. 2023;56(8):1794-1808. e8.
68. Suzuki K, Elegheert J, Song I, et al. A synthetic synaptic organizer protein restores glutamatergic neuronal circuits. *Science*. 2020;369(6507):eabb485.
69. Yuzaki M. The C1q complement family of synaptic organizers: not just complementary. *Curr Opin Neurobiol*. 2017;45:9-15.
70. Brown GC, Neher JJ. Microglial phagocytosis of live neurons. *Nat Rev Neurosci*. 2014;15(4):209-216.
71. Merkel PA, Jayne DR, Wang C, Hillson J, Bekker P. Evaluation of the safety and efficacy of Avacopan, a C5a receptor inhibitor, in patients with antineutrophil cytoplasmic antibody-associated vasculitis treated concomitantly with rituximab or cyclophosphamide/azathioprine: protocol for a randomized, double-blind, active-controlled, phase 3 trial. *JMIR Res Protoc*. 2020;9(4):e16664.
72. Vergunst CE, Gerlag DM, Dinant H, et al. Blocking the receptor for C5a in patients with rheumatoid arthritis does not reduce synovial inflammation. *Rheumatology(Oxford)*. 2007;46(12):1773-1778.

SUPPORTING INFORMATION

Additional supporting information can be found online in the Supporting Information section at the end of this article.

How to cite this article: Gomez-Arboledas A, Fonseca MI, Kramar E, et al. C5aR1 signaling promotes region- and age-dependent synaptic pruning in models of Alzheimer's disease. *Alzheimer's Dement*. 2024;20:2173-2190.
<https://doi.org/10.1002/alz.13682>